

A TWO-DIMENSIONAL DYNAMIC MODEL FOR A JAW MOVEMENT CONTROL ANALYSIS

Ken-ichi Itoh¹, Daisuke Ushiki², Hajime Murakami¹ and Toyohiko Hayashi³

¹Department of Information and Electronics Engineering, Niigata Institute of Technology, Niigata, Japan

²Graduate School of Engineering, Niigata Institute of Technology, Niigata, Japan

³Department of Biocybernetics, Faculty of Engineering, Niigata University, Niigata, Japan

Abstract—In order to clarify the control mechanism of a stomatognathic system, we developed a two-dimensional dynamic jaw model capable of performing an unloaded open-close movement. To simulate an open-close movement, we created a position feedback control scheme by providing a desired movement. Our numerical results verified that the proposed model could be applied to mandibular movement control analysis.

Keywords – dynamic model, control analysis, mandibular movement, constraint condition, computer simulation

I. INTRODUCTION

Stomatognathic functions such as chewing, swallowing, and speech are achieved by precise jaw movements, which are controlled by coordinated activities of the masticatory and suprahyoid muscles. During a jaw movement, these muscles must operate in a variety of ways, almost simultaneously. Additionally, the number of those involved in carrying out a given task is theoretically redundant.

To date, several investigations have been conducted in anatomy and physiology, though the control mechanism of these muscles has not yet been sufficiently clarified. Recently, numerical studies based on dynamic mathematical models and mastication robots have inspired interest [1],[2]. We previously analyzed the controllability of temporomandibular joint loading during biting by musculation, employing a simple static jaw model [3]. In this study, we developed a two-dimensional dynamic jaw model that included the morphology of the temporomandibular joint, and verified that the model could be applied to mandibular movement control analysis.

II. TWO-DIMENSIONAL DYNAMIC JAW MODEL

A. Outline

Let o - xy be a referential coordinate frame, where the origin o is fixed on the maxilla, and the x -axis is parallel to the Frankfort horizontal plane (Fig.1). The mandible and the maxilla were modeled as rigid masses, and the shape of the temporomandibular joint was represented as a third-order polynomial function. Our jaw model incorporated the following muscles: the masseter including the internal pterygoid, the superior and inferior lateral pterygoid, the anterior and posterior temporalis and digastric. The muscles

were assumed to run straight between their fixed origins in the maxilla and their fixed insertions in the mandible. The muscular-tendon was modeled using Hill's three-element model, referring to the musculoskeletal human body model of Komura et al. [4].

B. Constraint Equation

A third-order polynomial curve was used to represent the condylar movement path of the kinematic axis point :

$$a \cdot (-Xk + b) \cdot (-Xk - c)^2 - d \cdot Yk = 0 \quad (1)$$

where a, b, c, d denote arbitrary constants, and Xk, Yk denote the coordinates of the kinematic axis point (Fig. 1). The constraint equation can be derived by differentiating equation (1) with respect to time. Thus,

$$g_1 \cdot \dot{Xk} + g_2 \cdot \dot{Yk} = 0 \quad (2)$$

$$g_1 = -2 \cdot a \cdot (b - Xk) \cdot (-c - Xk) - a \cdot (-c - Xk)^2 \quad (3)$$

$$g_2 = -1$$

In vector-matrix notation, the equation (2) was expressed as:

$$Q(\underline{q})\dot{\underline{q}} = 0 \quad (4)$$

where $\underline{q} = [A_k, Xk, Yk]^T$, $Q(\underline{q}) = [0 \quad g_1 \quad g_2]$ and A_k is

the rotation angle of the mandible. This equation is embedded in the unconstrained dynamic equation.

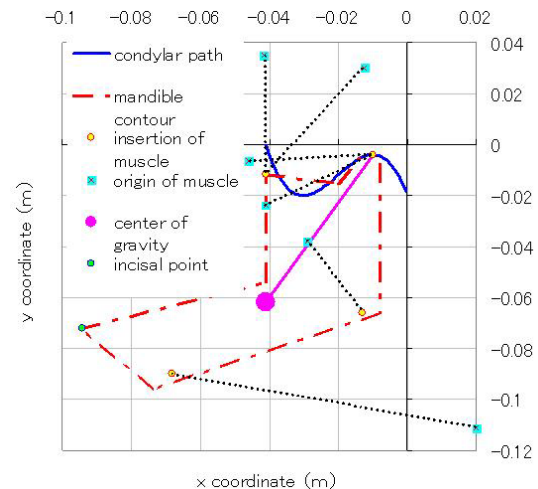


Figure 1. Two-dimensional jaw model including the morphology of the temporomandibular joint

Report Documentation Page

Report Date 25OCT2001	Report Type N/A	Dates Covered (from... to) -
Title and Subtitle A Two-Dimensional Dynamic Model for a Jaw Movement Control Analysis		Contract Number
		Grant Number
		Program Element Number
Author(s)	Project Number	
	Task Number	
	Work Unit Number	
Performing Organization Name(s) and Address(es) Department of Information and Electronics Engineering, Niigata Institute of Technology, Niigata, Japan		Performing Organization Report Number
Sponsoring/Monitoring Agency Name(s) and Address(es) US Army Research, Development & Standardization Group (UK) PSC 802 Box 15 FPO AE 0949-1500		Sponsor/Monitor's Acronym(s)
		Sponsor/Monitor's Report Number(s)
Distribution/Availability Statement Approved for public release, distribution unlimited		
Supplementary Notes Papers from the 23rd Annual International Conference of the IEEE Engineering in Medicine and Biology Society, October 25-28, 2001, Istanbul, Turkey. See also ADM001351 for entire conference on cd-rom., The original document contains color images.		
Abstract		
Subject Terms		
Report Classification unclassified	Classification of this page unclassified	
Classification of Abstract unclassified	Limitation of Abstract UU	
Number of Pages 4		

C. Dynamic Equation

The dynamic equation can be written as [5]:

$$A(\underline{q})\ddot{\underline{q}} - Q(\underline{q})\dot{\underline{q}}^2 = B(\underline{q})\dot{\underline{q}}^2 + C(\underline{q}) + M(\underline{q}) \quad (5)$$

where $A(\underline{q})$ is the mass matrix, $B(\underline{q})$ is the Coriolis and centrifugal effects, $C(\underline{q})$ is the gravitational term,

$$A(\underline{q}) = \begin{pmatrix} I + l^2 \cdot m & l \cdot m \cdot \cos(A_k) & l \cdot m \cdot \sin(A_k) \\ l \cdot m \cdot \cos(A_k) & m & 0 \\ l \cdot m \cdot \sin(A_k) & 0 & m \end{pmatrix}$$

$$B(\underline{q}) = \begin{pmatrix} 0 \\ -l \cdot m \cdot \sin(A_k) \\ l \cdot m \cdot \cos(A_k) \end{pmatrix} \quad C(\underline{q}) = \begin{pmatrix} -g \cdot l \cdot m \cdot \sin(A_k) \\ 0 \\ -g \cdot m \end{pmatrix},$$

$M(\underline{q}) \equiv [r_1, r_2, r_3]^T$ is the moment-arm matrix, $\underline{e} \equiv [e_1, e_2, e_3]$ is the constraint force, l is the distance between the kinematic axis point and the center of gravity, I is inertia, and g is gravitational force. If the equation (5) is premultiplied by the orthogonal compliment matrix $T(\underline{q})$ of $Q(\underline{q})$, it reduces to

$$T(\underline{q})A(\underline{q})\ddot{\underline{q}} = T(\underline{q})[B(\underline{q})\dot{\underline{q}}^2 + C(\underline{q}) + M(\underline{q})]. \quad (6)$$

Differentiating the constraint with respect to time gives an equation of the form

$$Q(\underline{q})\ddot{\underline{q}} = -\frac{\partial Q(\underline{q})}{\partial \underline{q}} \dot{\underline{q}}. \quad (7)$$

Embedding the constraint equation (7) in the dynamic equation (6), we get

$$\ddot{\underline{q}} = \begin{pmatrix} T(\underline{q})A(\underline{q}) \\ Q(\underline{q}) \end{pmatrix}^{-1} \begin{pmatrix} T(\underline{q})[B(\underline{q})\dot{\underline{q}}^2 + C(\underline{q}) + M(\underline{q})] \\ -\frac{\partial Q(\underline{q})}{\partial \underline{q}} \dot{\underline{q}} \end{pmatrix}. \quad (8)$$

III. EXPERIMENT

This section describes the simulation of an open-close movement, which was performed using a position feedback control scheme to provide a desired trajectory of the incisal point.

A. Position Control

Figure 2 shows the position feedback control system where t represents the update number, ΔZ is the weighted deviation, and K_i , K_p and K_s are the integral, proportional, and differential coefficients of the PID control system, respectively. Deviations between the desired position x_o, y_o and the incisal position x_{it}, y_{it} are weighted by coefficients A_s, B_s , and are input into the PID control system. The output of the PID control system is assumed to be the muscle activation level at . This activation exerts muscle force f_o^t .

B. Experimental Methods

First, the mandible was assumed to be static for 0.5s in a closing position. Subsequently, the open-close movement was carried out continuously for 10 repetitions. K_i , K_p and K_s were assumed to be 0.008, 50.0, and 0.2, respectively.

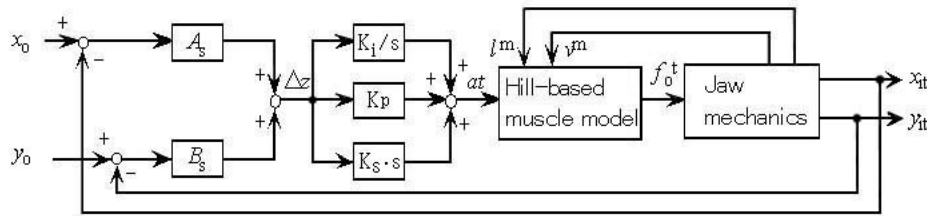


Figure 2. Position feedback control system

Table 1 lists the values of the weighted coefficients A_s, B_s and the initial muscle activation levels at . During the open-close movement simulation performed in this experiment, the activation level of the masseter including the internal pterygoid, which principally functions during biting, was always assumed to be $at = 0.0$.

C. Results and Discussion

The x - and y - coordinates of both the desired and the incisal trajectories are plotted against time in Fig. 3. Although the trajectory of the y -coordinate of the incisal point slightly vibrated, the incisal trajectories almost corresponded with the desired ones. Ten trajectories of the incisal point and the kinematic axis point are superimposed respectively and displayed in Fig. 4. The trajectories of the incisal point almost coincided except at the first open-close phase, and the trajectories of the kinematic axis point were on the third-order polynomial curve. From Fig. 3 and 4, it can be observed that our jaw model is capable of realizing an open-close movement with high reproducibility.

The muscle activation levels and muscle forces during the open-close movement are presented in Fig. 5 and Fig. 6. As shown in Fig. 5(a) and (b), the change patterns of activation levels between the first quarter and the last quarter differed. This probably means that the activation level changes assume a pattern suitable for the open-close movement by repeating the open-close movement continuously. The same tendency appeared in the change patterns of muscle forces.

As shown in Fig. 5(b), the activation level of the digastric muscle during the open phase showed a gradual rise, and levels of the anterior and posterior temporalis during the close phase showed gradual rises. The superior and inferior lateral pterygoids were active during both the open and close phases. These results agreed with the physiological data [2].

However, the muscle force of the digastric varied inversely with its activation level during the open phase. Because the digastric is a jaw-opening muscle, it is considered to be the exerting muscle force during the open phase. This is due to the nonlinear property of the Hill-based muscle model. The model is a function of muscle length, contraction velocity, and the muscle activation level. Even if the activation level increases, the muscle force cannot increase when the muscle length shortens with rapid speed. In future study, the muscle model needs to be improved [2].

IV. CONCLUSION

We developed a two-dimensional dynamic jaw model capable of performing an unloaded open-close movement, and carried out a position feedback control scheme by providing a desired movement. Throughout the experiment, it was verified that the two-dimensional dynamic jaw model was

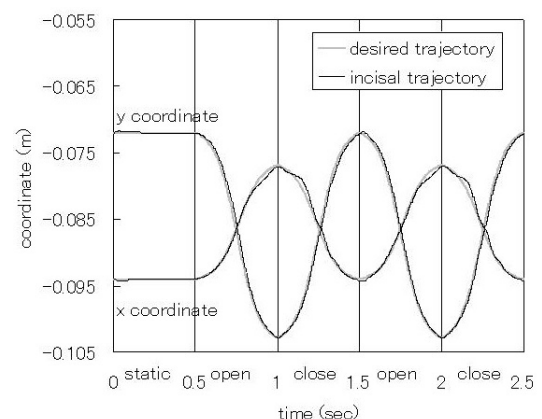
able to perform an open-close movement. The results of simulation also showed reasonably good agreement with physiological data [2]. We reached the conclusion that our jaw model could be applied to mandibular movement control analysis.

REFERENCES

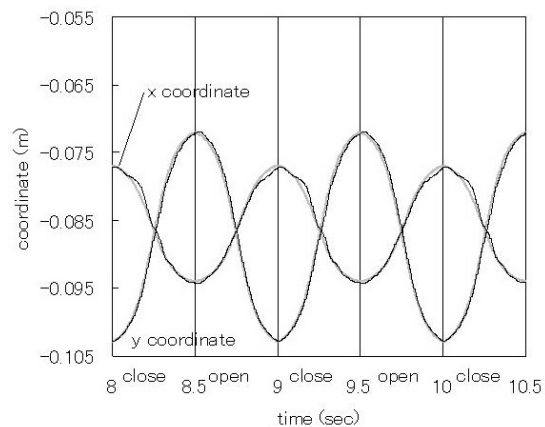
- [1] J.H.Koolstra and T.M.G.J. van Eijden, "The jaw open-close movements predicted by biomechanical modeling," *J.Biomechanics*, Vol.30, No.9, pp.943-950, 1997.
- [2] Shin-ichi Nakajima, Toyohiko Hayashi and Hiroshi Kobayashi, "Development of 2-D jaw movement simulator (JSN/S1)," *J. Robotics and Mechatronics*, Vol. 10, No. 6, pp.499-504, 1998.
- [3] Ken-ichi Itoh and Toyohiko Hayashi, "Functions of masseter and temporalis muscles in the control of temporomandibular joint loading –A static analysis using a two-dimensional rigid-body spring model," *Frontiers, Med. Biol. Engng.*, Vol.10, No.1, pp.17-31, 2000.
- [4] Taku Komura, Yoshihisa Shinagawa and Tosiya L. Kunii, "Muscle-based feed-forward controller of the human body," *Computer Graphics Forum*, 16(3), C165-C176, 1997.
- [5] Marcus G. Pandy, Felix E. Zajac, Eunsup Sim and William S. Levine, "An optimal control model for maximum-height human jumping," *J. Biomechanics*, Vol. 23, No. 12, pp.1185-1198, 1990.

Table 1. The values of the weighted coefficients A_s, B_s and the initial muscle activity levels

	A_s	B_s	at
daigstric	0.9	-0.3	0.1
inferior lateral pterygoid	-0.9	-0.45	0.12
masseter including internal pterygoid	0	0	0
anterior temporalis	0	0.9	0.25
superior lateral pterygoid	-0.3	-0.1	0.12
posterior temporalis	0.45	0.9	0.1

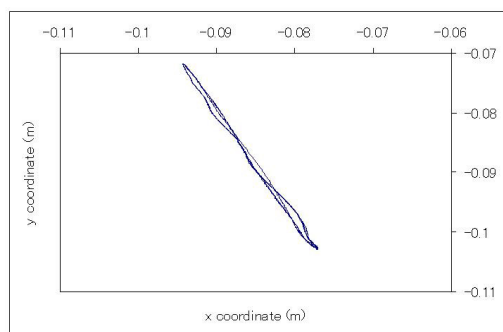


(a) The first quarter of jaw movement

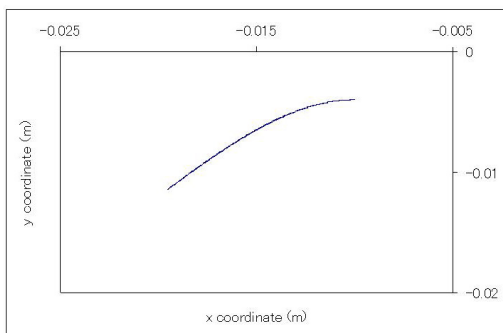


(b) The last quarter of jaw movement

Figure 3. x- and y- coordinates of both desired and incisal trajectories

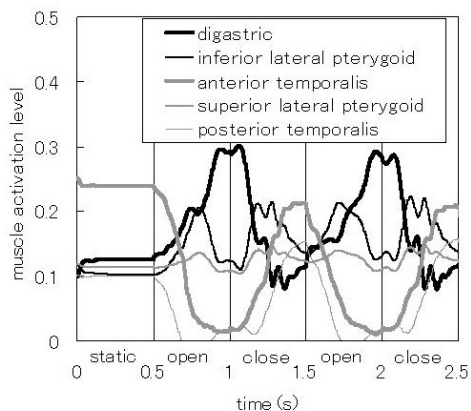


(a) Incisal point

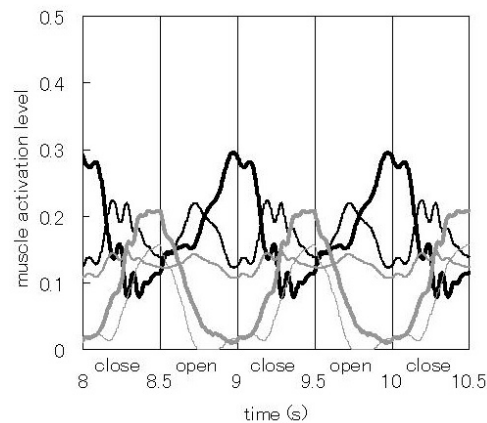


(b) Kinematic axis point

Figure 4. Trajectories of the incisal point and the kinematic axis point

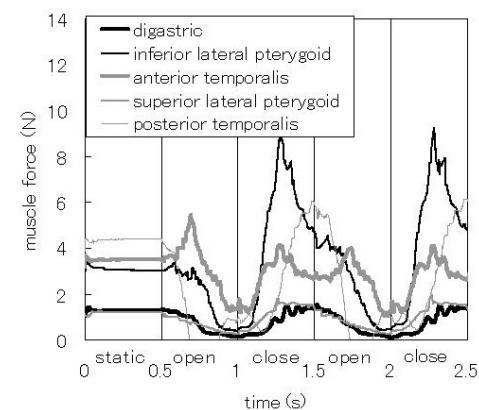


(a) The first quarter of jaw movement

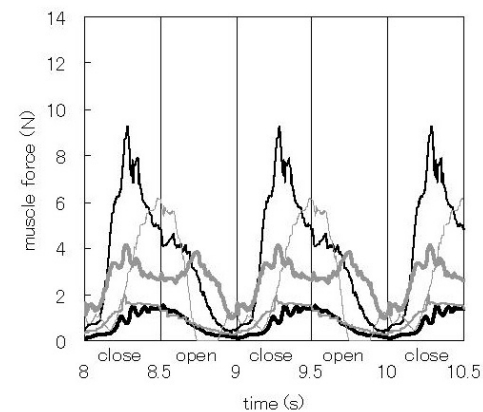


(b) The last quarter of jaw movement

Figure 5. Muscle activation levels plotted against time



(a) The first quarter of jaw movement



(b) The last quarter of jaw movement

Figure 6. Muscle forces plotted against time